RESEARCH ARTICLE | MAY 01 1987

Stabilization of flute modes by finite-Larmor-radius and surface effects

Maria Zales Caponi; Bruce I. Cohen; Robert P. Freis

Phys. Fluids 30, 1410–1415 (1987)
https://doi.org/10.1063/1.866254

Stabilization of flute modes by finite-Larmor-radius and surface effects

Maria Zales Caponi
Applied Technology Division, TRW, Inc., Redondo Beach, California 90278

Bruce I. Cohen and Robert P. Freis
Lawrence Livermore National Laboratory, University of California, Livermore, California 94550

(Received 24 October 1986; accepted 30 January 1987)

The combination of finite-ion-Larmor-radius effects and surface stabilization by contact with a lateral wall or with a line-tied cold-plasma blanket can stabilize interchange modes at low plasma beta (beta = plasma pressure/magnetic pressure) in axisymmetric mirror devices. This is illustrated analytically in a simple one-dimensional radial model and numerically with a two-dimensional stability code for anisotropic mirror plasmas and parameters appropriate to the TRW symmetric tandem mirror experiment [Phys. Fluids **28**, 1503 (1985)].

I. INTRODUCTION

Magnetohydrodynamic (MHD) stabilization of mirror plasmas by means other than nonaxisymmetric coil configurations (quadrupoles, baseball coils, yin–yang coil sets, surface multipoles, Ioffe bars) has been motivated by the cost of complicated magnetic coils and the deleterious effects on radial transport[1] of nonaxisymmetric systems. Axisymmetric configurations cannot satisfy the condition of absolute minimum $|B|$ that is necessary according to the simplest theories[2] to stabilize interchange modes. On the other hand, a number of mechanisms have been suggested to stabilize or partially stabilize flute modes in axisymmetric mirror devices and Q machines.[3–5] For example, it has recently been proposed that a close-fitting metallic wall can provide magnetohydrodynamic stability for a high-beta axisymmetric plasma (beta is the ratio of the plasma pressure to the vacuum magnetic pressure), because of the resistance to bending of magnetic field lines trapped between the plasma and a lateral conducting wall.[5] Here we theoretically examine how the combination of finite-ion-Larmor-radius effects and either a lateral conducting wall (or limiter), or a line-tied cold-plasma blanket can stabilize curvature-driven interchange modes in low-beta axisymmetric mirror or tandem mirror systems. This provides a possible stabilization mechanism to account for the enhanced MHD stability observed in the TRW symmetric tandem mirror experiment (STM)[6] and other low-beta axisymmetric experiments.[3,7]

The University of California at Irvine group directed by Professor N. Rynn has shown experimentally and theoretically how the combination of surface line tying and finite-ion-Larmor-radius (FLR) effects can stabilize flute modes in low-beta Q-machine plasmas in a series of papers.[3] Here, we use the recently developed FLORA axisymmetric tandem mirror stability code[8] to study the analogous physical situation in tandem mirrors using parameters characteristic of the TRW STM experiment. We also present a simple one-dimensional analytical calculation to illustrate the stabilization mechanism.[8] FLORA first calculates a two-dimensional (r,z), finite-beta, anisotropic plasma equilibrium with trapped- and passing-plasma components and multiple magnetic cells. The ensuing stability calculation incorporates FLR effects, $\mathbf{E}\times\mathbf{B}$ rotation, and the well-digging effects of hot rigid electrons,[6,8] if present. The validity of our analysis and the mathematical formulation of FLORA depend on the paraxial approximation and an expansion in the Larmor radius.[8,9]

Our principal results are that sharp reduction of low-beta interchange mode growth rates and complete stabilization are possible if FLR effects can rigidly attach the eigenmodes to the edge of the plasma, where either a lateral wall or surface line tying forces the perturbed transverse plasma displacement to zero. We determine that the ratio of the plasma pressure at the plasma/wall or plasma/blanket interface to the peak pressure on axis for stabilization is quite modest, 0.02–0.06 depending on the profile details for STM low-temperature streaming-plasma parameters. We have also investigated the stabilization's dependence on the shape of the pressure profile. Furthermore, we show that MHD stabilization is enhanced by increasing the pressure anisotropy $p_\perp/p_\parallel$, which allows the fraction of hot plasma extending to the lateral wall to be decreased further.

II. STABILITY ANALYSIS

A simple one-dimensional eigenequation describing low-beta flute stability including rotation, FLR, and anisotropy effects was derived in Ref. 8 for systems with weak axial variation

$$\frac{1}{r}\frac{\partial}{\partial r}\left(\rho T r^3 \frac{\partial}{\partial r}\xi\right) + (1-m^2)\rho T\xi + r\omega^2\xi\frac{\partial}{\partial r}\rho - m^2 k\xi\frac{\partial}{\partial r}(p_\perp + p_\parallel) = 0\,, \tag{1}$$

where ξ is the perturbed radial displacement, m is the azimuthal mode number, $k = \partial^2 r/\partial z^2$ is the magnetic field-line curvature, ρ is the mass density, $p_\perp$ and $p_\parallel$ are the pressure components, and

$$T = \sum_s \rho_s[\omega^2 - m\omega(\Omega_1+\Omega_2) + m^2\Omega_1\Omega_2]_s\,. \tag{2}$$

For a rotating isothermal Maxwellian plasma, $\Omega_1 = \Omega_E + \Omega_*$ and $\Omega_2 = \Omega_E + \Omega_{\nabla B}$, where Ω_E, Ω_*, and $\Omega_{\nabla B}$ are the $\mathbf{E}\times\mathbf{B}$, diamagnetic, and ∇B angular drift velocities, respectively, for the species denoted by the subscript s,

 0031-9171/87/051410-06$01.90

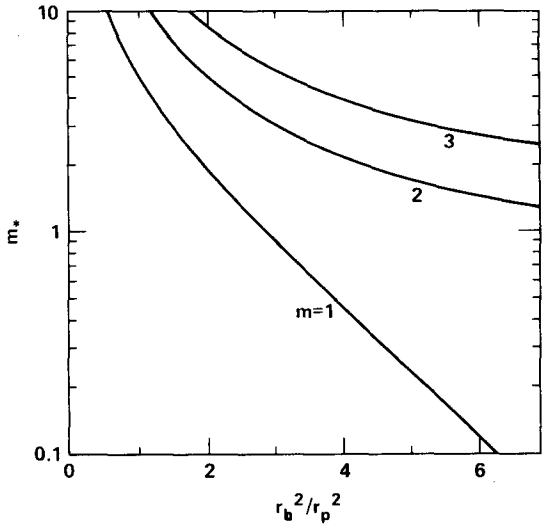

FIG. 1. The eigenvalue relation for m_* as a function of r_b^2/r_p^2 for the lowest radial mode and $m = 1$, 2, and 3, where r_p is the e-folding radius of the Gaussian pressure and density profiles, and r_b is the radius where the radial plasma displacement vanishes.

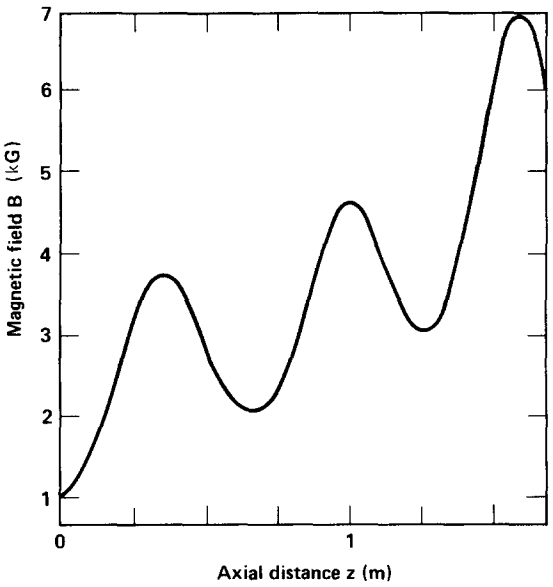

FIG. 2. Model axial magnetic field for numerical study of the TRW symmetric tandem mirror experiment.

$$\Omega_E = \frac{c}{rB}\frac{\partial\phi}{\partial r}, \quad \Omega_* = \frac{m_s c}{re_s B\rho_s}\frac{\partial p_{\perp s}}{\partial r}, \quad \Omega_{\nabla B} = \frac{m_s c p_{\perp s}}{re_s B\rho_s}\frac{\partial \ln B}{\partial r}. \tag{3}$$

With radial profiles, $p_\perp + p_\parallel = p_0(1+\alpha)\exp(-r^2/r_p^2)$ and $\rho = \rho_0 \exp(-r^2/r_p^2)$, and $\Omega_E = \text{const}$, where $\alpha \equiv p_\perp/p_\parallel$, a simple change of variables transforms Eq. (1) to Whittaker's equation.[3,8,10] For insulating axial boundary conditions $\partial\xi/\partial z = 0$, and complete stabilization $\xi = 0$ at the radial location r_b of a conducting wall, limiter, or line-tied plasma blanket, solutions are obtained in terms of Whittaker and Kummer functions. The eigenfrequencies are given by[8]

$$\omega = \frac{mm_*(\Omega_1+\Omega_2)}{2(1+m_*)} \pm \frac{m}{2(1+m_*)}\left[m_*^2(\Omega_1+\Omega_2)^2 - 4(1+m_*)(m_*\Omega_1\Omega_2 + \Gamma^2)\right]^{1/2}, \tag{4}$$

where $\Gamma^2 = -kp_0(1+\alpha)/r\rho_0$ and is independent of r at low beta because k is proportional to r, and m_* is a geometrical factor determined by the eigenvalue condition derived from the vanishing of the displacement at the radial boundary. The eigenvalue condition is

$$M[(m - m_* - 1)/2, m+1, r_b^2/r_p^2) = 0,$$

where M is Kummer's function.[8] The resulting value for m_* is an increasing function of m and is a decreasing function of the relative wall radius r_b/r_p (see Fig. 1). For $r_b/r_p \to \infty$, $m_* \to m-1$ for the lowest radial mode.

The overall stabilizing effect of the $\xi = 0$ boundary condition at $r = r_b$ is easily deduced from Eq. (4) and the dependence of m_* on r_b/r_p. For $r_b^2/r_p^2 < 3$, then $m_* > 1$ for all m and there is a geometrical reduction of Im ω below Γ, the MHD growth rate in the absence of FLR and rotation. Rotational instability can emerge from the $-\Omega_1\Omega_2$ term under the square root, and FLR stabilization derives from the non-negative $(\Omega_1+\Omega_2)^2$ term. For the simple case of $\Omega_E = 0$ and low beta so that $|\Omega_{\nabla B}/\Omega^*| \ll 1$, then $\Omega_1 \approx \Omega_*$ and $\Omega_2 \approx 0$. In this limit the stability condition resulting from Eq. (4) is

$$m_*^2\Omega_*^2 - 4(1+m_*)\Gamma^2 \geqslant 0. \tag{5}$$

We see in (5) that the FLR stabilization depends strongly on the geometry through m_*. We also note that Eq. (4) indicates that the eigenfrequency for unstable modes acquires a real part for finite $m_*(\Omega_1+\Omega_2)$. Qualitatively similar results were obtained earlier by Lehnert, who analytically investigated low-beta electrostatic flutes in an axially uniform system with a plane slab boundary and a gravitational field.[11]

Our analysis is motivated by observations in the TRW STM experiments, in which particle and energy confinement times $\tau_p \gtrsim 100\,\mu$sec and $\tau_e \geqslant 50\,\mu$sec were obtained that were significantly greater than the predicted MHD growth times $\gamma_{\text{MHD}}^{-1} \lesssim 10\,\mu$sec.[12] Fluctuation measurements showed spectral peaks at several frequencies below 50 kHz for ion cyclotron heated plasmas with $T_i \sim 0.8$ keV. The ion diamagnetic frequency Ω_* for these plasmas was of order 10^6 rad/sec, i.e., $\Omega_* \gtrsim 10\,\gamma_{\text{MHD}}$. Equation (4) suggests that substantial reduction of the MHD growth rate then requires $m_* \gtrsim 0.2$ corresponding to $r_b^2/r_p^2 \lesssim 6$ for $m = 1$ and results in a frequency $\text{Re}\,\omega/2\pi = m_*\Omega_*/4\pi(1+m_*) \gtrsim 20$ kHz. The value $r_b^2/r_p^2 \sim 6$ corresponds to a ratio of the density or pressure at r_b to the peak value on axis of $< 10^{-2}$.

The stabilization mechanism was further investigated numerically using the FLORA code with parameters characteristic of the STM experiment. The axial vacuum magnetic field profile used to model STM is shown in Fig. 2. Radial pressure and density profiles for isothermal plasma components were modeled functionally by

$$p(\psi) = \tfrac{1}{2}p_0[1 - \tanh(2(\psi - \psi_0)/\Delta\psi)]. \tag{6}$$

In Fig. 3 are plotted model profiles for $p_\perp$ as functions of z and the magnetic flux ψ for passing-plasma ($p_\perp \sim p_\parallel$) and

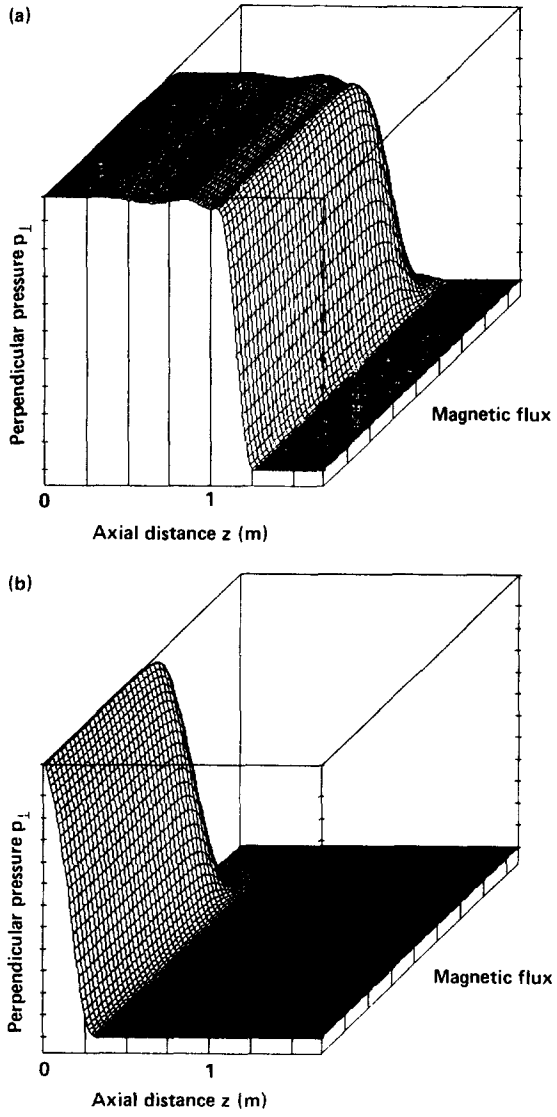

FIG. 3. Model perpendicular pressure profiles as functions of axial position z and magnetic flux ψ for (a) passing-plasma ($p_\perp \sim p_\parallel$) dominated cases and (b) trapped-plasma ($p_\perp \sim 3p_\parallel$) cases.

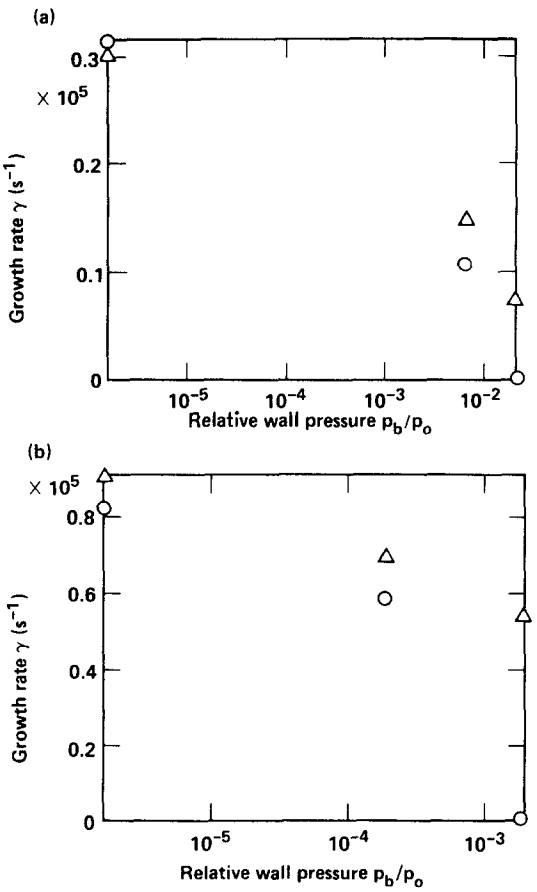

FIG. 4. Growth rates γ for $m = 1$ flute modes as a function of p_b/p_0 for passing plasmas with (a) $\beta_\perp = 2\times10^{-4}$ and (b) $\beta = 0.05$ at maximum. Results with FLR are indicated by O and with no FLR by △.

trapped-plasma ($p_\perp \sim 3p_\parallel$) dominated low-beta equilibria. The parallel and perpendicular pressure profiles satisfy parallel force balance.[8,9]

Figure 4(a) presents growth rates $\gamma \equiv \mathrm{Im}\,\omega$ for unstable $m = 1$ flutes as a function of p_b/p_0, the ratio of the perpendicular pressure component at the radial boundary to its axial value, for $\Delta\psi/\psi_0 = 0.2$. The values of p_b/p_0 were changed by varying ψ_0 in Eq. (6). All the plasma was taken to be passing with a peak passing-plasma perpendicular beta $\beta_p = 2\times10^{-4}$; the pressure was isotropic; and the peak density was $n_p = 4\times10^{11}\ \mathrm{cm}^{-3}$ corresponding to a temperature of 50 eV. These conditions simulate the streaming-plasma operation in the STM experiment. At this very low plasma beta, for which beta is less than the square of the long-thin parameter, the transverse gradient of the magnetic field is negligible within the limits set by the paraxial theory. Therefore, the ∇B drift frequency is negligible in our stability calculation. However, the diamagnetic and $\mathbf{E}\times\mathbf{B}$ drift frequencies can be finite; and our stability theory remains valid with $\Omega_E, \Omega_* \neq 0$ and $\Omega_{\nabla B} = 0$. The growth rates with and without stabilizing FLR are shown in Fig. 4(a). For all of our FLORA cases $\Omega_E = 0$ and $|\Omega_{\nabla B}/\Omega_*| \to 0$. We observed that complete stabilization occurred for $p_b/p_0 \sim 0.02$ with FLR. With no FLR there was instability. In the presence of FLR the modes acquired a real frequency $\mathrm{Re}\,\omega \sim \Omega_*$, and $\mathrm{Re}\,\omega$ increased with increasing p_b/p_0.

Instability accompanied disconnecting the plasma from the lateral boundary by cutting off the profile. Furthermore, there was also instability when the plasma pressure profile was flat as it approached the lateral boundary. In both of these examples, the FLR effects needed to connect the stabilizing boundary to the eigenmode interior to the plasma vanished before reaching the boundary because $\Omega_* \propto \partial p_\perp/\partial r \to 0$. The stabilizing boundary influences the core of the low-beta plasma when the pressure gradient and, hence, Ω_* are finite all the way to the boundary. As the peak of the MHD pressure-weighted curvature drive was moved closer to the stabilizing boundary in our numerical studies, there was increased stabilization. Part of the stabilization derived from the foot of the pressure profile being removed, which decreased the MHD drive [Fig. 5(a)]. However, complete stabilization was achieved with the peak of the field-line-averaged local MHD growth rate remaining well inside the radial boundary. Figure 5(b) presents the radial eigenfunction profile for a partially FLR-stabilized $m = 1$ flute and

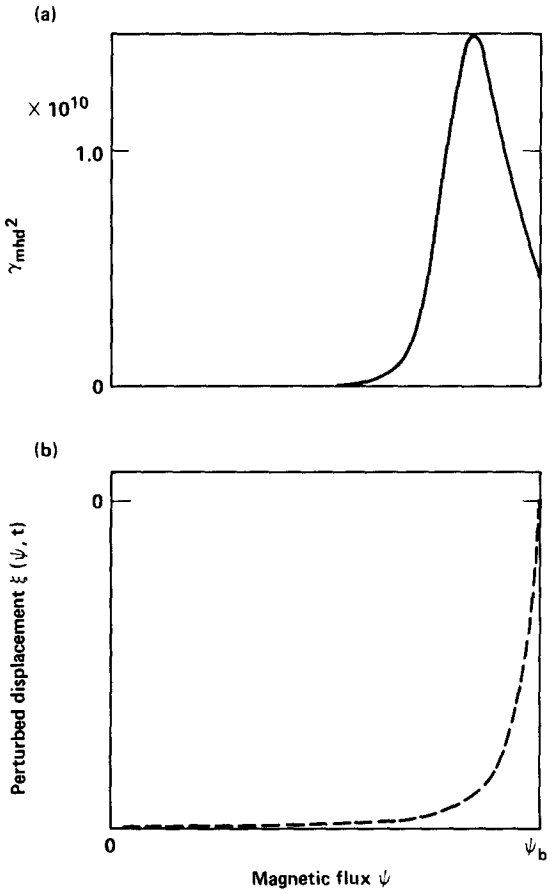

FIG. 5. (a) The flux-tube averaged infinite-m flute-mode growth rate squared as a function of flux ψ. (b) The instantaneous radial eigenfunction $\xi(\psi,t)$ as a function of flux for an $m=1$ flute mode with FLR. The plasma parameters were $\beta_p = 2\times10^{-4}$ and $n_p = 5\times10^{11}$ cm^{-3} on axis with $p_b/p_0 = 6.7\times10^{-3}$.

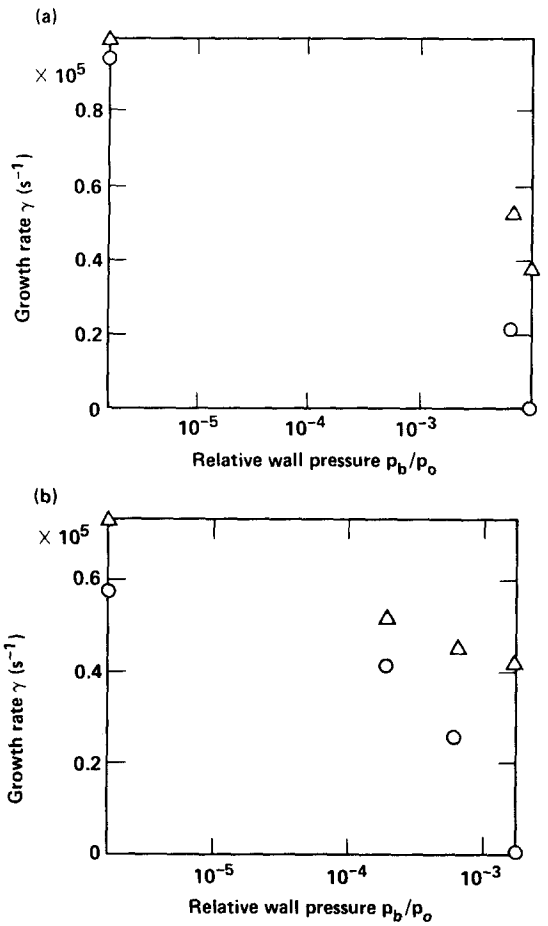

FIG. 6. Growth rates γ for $m=1$ flute modes as a function of p_b/p_0 for $\beta = 10^{-4}$ and $n_p = 5\times10^{11}$ cm^{-3} at maximum, with (a) $\beta_{\perp c} = 0.005$, $n = 5\times10^{11}$ cm^{-3} and (b) $\beta_{\perp c} = 0.05$, $n_c = 5\times10^{12}$ cm^{-3} at maximum, an with (○) and without (△) FLR effects.

shows the relative flatness of the eigenmode inside the plasma.

To investigate the influence of pressure-profile modification, we varied $\Delta\psi$ and ψ_0 for fixed $p_b/p_0 = 6.7\times10^{-3}$ and the same low-beta streaming-plasma parameters described earlier. Over a range $0.1\leqslant\Delta\psi/\psi_0\leqslant0.3$, where $\psi_0 = r_0^2B/2$, FLR effects produced significant partial stabilization. The slope of the pressure profile increased in magnitude with decreasing $\Delta\psi/\psi_0$; this in turn linearly increased $\gamma^2_{\rm MHD}$ and quadratically increased Ω_*^2. Because p_b/p_0 was fixed, we had to increase ψ_0/ψ_b as we decreased $\Delta\psi/\psi_0$. Thus, the effective m_* for these profiles probably did not decrease as much as Ω_*^2 increased with decreasing $\Delta\psi/\psi_0$. The final result was that FLR stabilization improved for the steeper profiles: the observed $m=1$ growth rate was 1.58×10^4 sec^{-1} for $\Delta\psi/\psi_0 = 0.3$ and 1.07×10^4 sec^{-1} for $\Delta\psi/\psi_0 = 0.2$. There was stability for $\Delta\psi/\psi_0 = 0.1$.

Wall and FLR stabilization persisted at higher passing-plasma betas. Figure 4(b) shows $m=1$ growth rates obtained for peak $\beta_p = 0.05$, peak $n_p = 5\times10^{12}$ cm^{-3}, and $T_i \sim 1$ keV. Here, complete stabilization occurs at a lower value of $p_b/p_0 \sim 0.002$ than the corresponding value for lower β_p. Although the MHD drive has significantly increased, because of the increase in temperature ($\gamma^2_{\rm MHD}\propto T_i$), Ω_*^2 increases more rapidly ($\Omega_*^2\propto T_i^2$) so that the geometrical enhancement factor m_* need not be as large. As in th previously described lower-beta cases, Re ω increased witl increasing p_b/p_0 and, hence, increasing effective value o m_*. Furthermore, Re $\omega \ll \Omega_*$ which is consistent with a effective m_* much smaller than 1. The addition of a uniform cold background plasma ($T=0$) with $n_c = 10^{11}$ cm^{-3} which was 2% of n_p on axis but was comparable to or ex ceeded the passing-plasma density at the lateral boundar depending on parameters, had no significant effect on th observed growth rates and the marginal stability point. Th cold background plasma insured that the temperature of th edge plasma as a whole was low.

We also modeled a magnetically trapped plasma com ponent similar to the plasma created by ion cyclotron heat ing in the central cell of STM. The equilibrium trapped plas ma had significant anisotropy: $p_\perp/p_\parallel \sim 3$ was used in FLORA Anisotropy is expected to modify the competition betwee the pressure-weighted curvature drive and the FLR stabili zation in the following manner. In Eqs. (4) and (5) we not that the MHD drive is proportional to $\partial(p_\perp + p_\parallel)/\partial\psi$ an that Ω_*^2 is proportional to $(\partial p_\perp/\partial\psi)^2$. Hence, increasin $p_\perp/p_\parallel$ is expected to enhance the relative strength of the FLR stabilization, and the FLR stabilization remains quite sensi tive to the relative position of the lateral boundary. Further

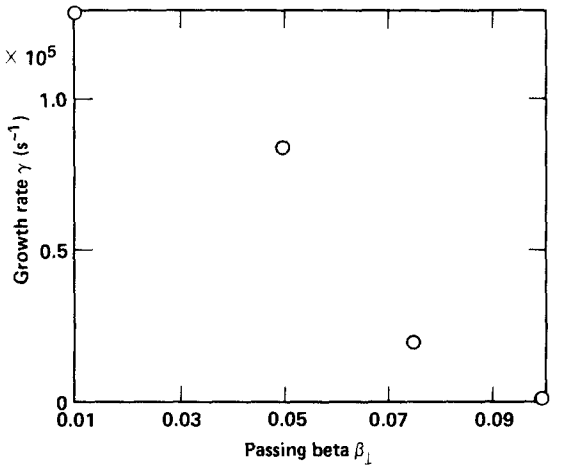

FIG. 7. Growth rates γ for $m = 1$ flute modes as a function of $\beta_{\perp p}$ with $p_b/p_0 = 1.6\times10^{-6}$, $\beta_{\perp c} = 0$, a fixed temperature of 1 keV, and FLR effects.

more, the axial weighting of regions of good and bad curvature by the trapped plasma differs significantly from that by passing plasma because of their different axial distributions. This is reflected by the field-line-averaged values of $\gamma^2_{\rm MHD}$.

To illustrate the effects of anisotropy, we compare the stability of the following two cases corresponding to tandem mirror configurations as diagrammed in Figs. 2 and 3. In the first case there was only passing plasma with $p_b/p_0 = 1.89\times10^{-4}$, and peak values $\beta_\perp = \beta_\parallel = 5\times10^{-2}$ and $n_p = 5\times10^{12}$ cm^{-3} on axis. The observed growth rate was 5.8×10^4 sec^{-1} with FLR included and $\gamma^2_{\rm MHD} = 2.4\times10^{11}$ sec^{-2}. In the second case there was only trapped plasma with $\beta_\perp = 3\beta_\parallel = 5\times10^{-2}$ on axis and otherwise the same parameters. The observed growth rate with FLR was reduced to 4.5×10^4 sec^{-1}, although $\gamma^2_{\rm MHD} = 6.95\times10^{11}$ was significantly increased by the different axial weighting.

For the $m = 1$ growth rates observed in FLORA and plotted in Figs. 6(a) and 6(b), the peak perpendicular betas for the trapped plasma in the center cell were $\beta_{\perp c} = 0.005$ and 0.05, the peak trapped plasma densities were $n_c = 5\times10^{11}$ and 5×10^{12} cm^{-3}, respectively. These parameters correspond to center cell ion temperatures at 1 keV. For the passing-plasma present, $\beta_p = 10^{-4}$ and $n_p = 5\times10^{11}$ cm^{-3} at maximum. The observed growth rates with FLR were $\sim$30% smaller for the trapped-plasma cases than for the streamimg-plasma cases examined earlier with the same peak perpendicular beta [Figs. 4(b) and 6(b)]. Complete stabilization occurred for $p_b/p_0 \sim 0.002$–0.007. The observed oscillation frequencies for the $m = 1$ unstable modes were much reduced below Ω_* (Re $\omega/2\pi \lesssim 8$ kHz) indicating an effective $m_* \ll 1$, and Re ω decreased with decreasing p_b/p_0 as in the earlier cases.

Numerical studies with FLORA indicate that the combination of wall and FLR stabilization persists for moderately large $\beta_\perp$ values, e.g., $\beta_{\perp p} \gtrsim 0.1$, if the plasma remains in contact with a wall that is not too distant (Fig. 7). This can be understood as follows. At finite $\beta_\perp$,

$$\Omega_{\nabla B} \sim -[\beta_\perp/2(1-\beta_\perp)]\Omega_* ;$$

and $\Omega_{\nabla B}$ must be retained in Eqs. (2) and (4). For the purpose of this simple discussion, we continue to omit ballooning effects; of course, ballooning issues must be addressed at high beta. If Ω_E remains negligible, i.e., $|\Omega_E| \ll |\Omega_*|, |\Omega_{\nabla B}|$, then the quasielastic term[8,9] $\Omega_1\Omega_2 = \Omega_*\Omega_{\nabla B}$ in the discriminant of Eq. (4) is now finite, negative, and stabilizing. The square of the gyroscopic term[8,9] in the discriminant, $(\Omega_1+\Omega_2)^2 = (\Omega_* + \Omega_{\nabla B})^2$, remains positive and stabilizing, but is reduced in magnitude. For plasma beta values well below the limits set by the mirror mode, the failure of the paraxial approximation, and the onset of ballooning, increasing the plasma beta increases the curvature drive $\Gamma^2 \propto \beta_\perp + \beta_\parallel$, while the stabilization increases faster: $\Omega_1\Omega_2 \propto -\beta_\perp^3(1-\beta_\perp)^2$ and the terms contributing to $(\Omega_1+\Omega_2)^2$ increase at least as fast as $\beta_\perp^2$. Here we note the obvious effect of anisotropy on stability.

It has been suggested that the foregoing arguments may have accounted for the observed transition from an unstable to a stable plasma when the radially averaged plasma betas were increased from 0.35 to 0.45 in the University of California axisymmetric mirror experiment.[13] Numerical evaluations of Eq. (4) are consistent with the experimental observations in Ref. 13 if we assume $|\Omega_E| \ll |\Omega_*|, |\Omega_{\nabla B}|$ and use a reasonable value of $(r_b/r_p)^2 = 4$, which gives a value of $m_* = 0.5$ for $m = 1$. There is some data indicating that the radial potential profile was fairly flat in the experiment to support the assumption that Ω_E is small. If Ω_E is comparable to or greater than Ω_* and $\Omega_{\nabla B}$, Eq. (4) must be analyzed more generally; and the results differ significantly from the case with $\Omega_E = 0$.[8]

III. CONCLUSIONS

Our analysis and the numerical results using the FLORA code confirm and extend earlier experimental and theoretical studies indicating that low-beta MHD flute modes can be stabilized by a stabilizing lateral boundary condition if FLR effects in the plasma extend to the surrounding stabilized boundary. The fractional plasma pressures (and pressure gradients) at the boundary are quite modest, a few percent or less depending on parameters and profile details. Our numerical studies using parameters characteristic of the STM experiment suggest that the combination of FLR and surface stabilization is a viable mechanism for the enhanced MHD stability observed in the experiment. The small fractions of plasma pressure required at the surface for significant stabilization are reasonable, and the oscillation frequencies observed in FLORA are in the same range as the STM experimental observations. Finally, our results indicate that the combination of FLR and surface stabilization persists for increasing beta values and may account for the observed MHD stability of the University of California axisymmetric mirror experiment at average beta values equal to 0.45. This suggests the possible use of a cold-plasma line-tied blanket to afford stability during the build-up phase to a high-beta wall-stabilized axisymmetric plasma that is completely detached from the stabilizing boundary.

ACKNOWLEDGMENTS

We thank N. H. Lazar, A. J. Lichtenberg, L. D. Pearlstein, W. A. Newcomb, and J. J. Thomson for valuable discussions, support, and encouragement.

The work of M. Z. Caponi was supported by the U. S. Department of Energy under Contract No. DE-AC03-85ER51089 at TRW, Inc. The research of B. I. Cohen and R. P. Freis was performed at Lawrence Livermore National Laboratory under the auspices of the U. S. Department of Energy under Contract No. W-7405-ENG-48.

[1]D. D. Ryutov and G. V. Stupakov, Fiz. Plazmy **4**, 501 (1978) [Sov. J. Plasma Phys. **4**, 278 (1978)]; R. H. Cohen, Comments Plasma Phys. Controlled Fusion **4**, 157 (1979).

[2]Yu. T. Baiborodov, M. S. Ioffe, V. M. Petrov, and R. I. Sobolev, Sov. J. At. Energy **14**, 459 (1964); J. B. Taylor, Phys. Fluids **7**, 767 (1964).

[3]S. Fornaca, Y. Kiwamoto, and N. Rynn, Phys. Rev. Lett. **42**, 772 (1979); D. Segal, M. Wickham, and N. Rynn, Phys. Fluids **25**, 1485 (1982); D. Segal, *ibid.* **26**, 2565 (1983); and references therein.

[4]G. E. Guest, R. L. Miller, and M. Z. Caponi, Phys. Fluids **29**, 2556 (1986).

[5]H. L. Berk, M. N. Rosenbluth, H. V. Wong, and T. M. Antonsen, Jr., Phys. Fluids **27**, 2705 (1984); T. B. Kaiser and L. D. Pearlstein, *ibid.* **28**, 1003 (1985); G. R. Smith, H. L. Berk, and L. L. LoDestro, *ibid.* **29**, 1798 (1986).

[6]B. H. Quon, R. A. Dandl, W. DiVergilio, G. E. Guest, L. L. Lai, N. H. Lazar, T. K. Samec, and R. F. Wuerker, Phys. Fluids **28**, 1503 (1985).

[7]R. F. Post, R. E. Ellis, F. C. Ford, and M. N. Rosenbluth, Phys. Rev. Lett. **11**, 166 (1960); see AIP Document No. PAPS PFLDA-29-1558-336 for 336 pages of *Status of Mirror Fusion Research 1980*, edited by B. I. Cohen. Order by PAPS number and journal reference from American Institute of Physics, Physics Auxiliary Publication Service, 335 East 45th St., New York, NY 10017. The price is $1.50 for each microfiche (98 pages) or $5.00 for photocopies of up to 30 pages, and $0.15 for each additional page over 30 pages. Airmail additional. Make checks payable to the American Institute of Physics.

[8]B. I. Cohen, R. P. Freis, and W. A. Newcomb, Phys. Fluids **29**, 1558 (1986).

[9]W. A. Newcomb, J. Plasma Phys. **26**, 529 (1981); Phys. Fluids **28**, 505 (1985).

[10]M. N. Rosenbluth, N. A. Krall, and N. Rostoker, Nucl. Fusion Suppl. Pt. 1, 143 (1962); T. D. Rognlien, J. Appl. Phys. **44**, 3505 (1973).

[11]B. Lehnert, Phys. Fluids **9**, 1367 (1966).

[12]T. Christensen, S. Talmadge, and N. H. Lazar, Bull. Am. Phys. Soc. **30**, 1436 (1985).

[13]R. M. Close, B. K. Kang, A. J. Lichtenberg, M. A. Lieberman, and H. Meuth, Phys. Fluids **29**, 3892 (1986).